Journal of Power Sources 195 (2010) 6116–6121

Contents lists available at ScienceDirect

Journal of Power Sources

journal homepage: www.elsevier.com/locate/jpowsour

Effect of phase inversion on microporous structure development of Al_2O_3/poly(vinylidene fluoride-hexafluoropropylene)-based ceramic composite separators for lithium-ion batteries

Hyun-Seok Jeong [a], Dong-Won Kim [b], Yeon Uk Jeong [c], Sang-Young Lee [a,*]

[a] Department of Chemical Engineering, Kangwon National University, Hyoja2-dong, Chuncheon, Kangwondo 200-701, Republic of Korea
[b] Department of Chemical Engineering, Hanyang University, Seoul 133-791, Republic of Korea
[c] School of Materials Science and Engineering, Kyungpook National University, Daegu 702-701, Republic of Korea

ARTICLE INFO

Article history:
Received 12 September 2009
Received in revised form 22 October 2009
Accepted 29 October 2009
Available online 10 November 2009

Keywords:
Lithium-ion batteries
Safeties
Separators
Thermal shrinkage
Ceramic coating layers
Phase inversion

ABSTRACT

To improve the thermal shrinkage of the separators that are essential to securing the electrical isolation between electrodes in lithium-ion batteries, we develop a new separator based on a ceramic composite membrane. Introduction of microporous, ceramic coating layers onto both sides of a polyethylene (PE) separator allows such a progress. The ceramic coating layers consist of nano-sized alumina (Al_2O_3) powders and polymeric binders (PVdF-HFP). The microporous structure of the ceramic coating layers is observed to be crucial to governing the thermal shrinkage as well as the ionic transport of the ceramic composite separators. This microporous structure is determined by controlling the phase inversion, more specifically, nonsolvent (water) contents in the coating solutions. To provide a theoretical basis for this approach, a pre-investigation on the phase diagram for a ternary mixture comprising PVdF-HFP, acetone, and water is conducted. On the basis of this observation, the effect of phase inversion on the morphology and air permeability (i.e. Gurley value) of ceramic coating layers is systematically discussed. In addition, to explore the application of ceramic composite separators to lithium-ion batteries, the influence of the structural change in the coating layers on the thermal shrinkage and electrochemical performance of the separators is quantitatively identified.

1. Introduction

As the demands for higher power-density and higher energy-density lithium-ion batteries continue to grow, the accompanying safety concerns are issued as a critical challenge. From the viewpoint of battery safety failures, a separator is considered a key component to secure battery safety, because its primary function is to keep the physical isolation between a cathode and an anode of a battery so that no electrons can flow between them [1]. In general, separators in lithium-ion batteries are made mostly of polyolefins, usually polyethylene (PE) or polypropylene (PP). Though these polyolefin-based separators are widespread and have many advantages, their poor thermal shrinkage and mechanical strength have raised serious concerns with their ability to maintain the necessary electrical isolation between electrodes, particularly under vigorous conditions such as abnormal heating or mechanical rupture. Recently, a variety of approaches for overcoming these technical drawbacks of polyolefin-based separators have been investigated, including polymer electrolyte-modified separators [2–4], self-standing inorganic separators [5,6], polyethylene terephthalate (PET) nonwoven-inorganic composite separators [7], nonwoven fabrics consisting of para-phenylene terephthalamide (PPTA) fibers [8], and nanofiber-based separators prepared by electrospinning [9,10]. Among these alternatives, the use of inorganic layers has drawn great attention because of their superiority in suppressing the thermal shrinkage and mechanical breakdown of separators.

In this study, as a new approach to significantly improve the thermal shrinkage of a separator, we develop a ceramic composite separator featuring ceramic coating layers with microporous structures that are applied onto both sides of a PE separator. The ceramic coating layers consist of nano-sized alumina (Al_2O_3) powders and polymeric binders (PVdF-HFP). Meanwhile, to provide a theoretical basis for controlling the microporous structure of the ceramic coating layers, a pre-investigation on the phase inversion for a ternary mixture comprising the polymer (PVdF-HFP), solvent (acetone), and nonsolvent (water) was conducted. Phase inversion is known to be an effective way to develop porous structures in membranes, where a competitive mutual diffusion between solvent and nonsolvent occurs to yield porous structures [11–13]. On the basis of

* Corresponding author. Tel.: +82 33 250 6338; fax: +82 33 251 3658.
E-mail address: syleek@kangwon.ac.kr (S.-Y. Lee).

0378-7753/$ – see front matter © 2009 Elsevier B.V. All rights reserved.
doi:10.1016/j.jpowsour.2009.10.085

this observation, the effect of phase inversion, more specifically, of the nonsolvent (water) contents in the coating solutions, on the microporous structure development of the ceramic coating layers is systematically discussed. In addition, the influence of this structural change in the coating layers on the thermal shrinkage and electrochemical performance of the ceramic composite separators is quantitatively identified.

2. Experimental

A solution for ceramic coating layers was prepared by mixing Al_2O_3 nanoparticles (average particle size = 480 nm) and PVdF-HFP (HFP content = 6 mol%) in acetone as a solvent, where a composition ratio of Al_2O_3/PVdF-HFP was fixed at 50/50 (w/w). After dissolving PVdF-HFP in acetone, a fixed amount of Al_2O_3 powders was added and the solution was further subjected to vigorous mixing via bead-milling for 2 h. To induce and control the phase inversion of the coating solutions, a pre-determined amount of water (nonsolvent) was slowly added into the solution, where the water content in the solution was varied from 1.89 wt% to 9.43 wt%. As a coating substrate, a microporous PE separator (F20BHE, thickness = 20 μm, Gurley value = 240 s/100 cm^3, porosity = 45%, ExxonMobil Chemical) was chosen. By employing a dip-coating process, the coating solution was applied onto both sides of a PE separator. The separator was then dried at room temperature in order to evaporate the acetone and further vacuum dried at 50 °C for 4 h. The final thickness of the ceramic composite separators was controlled to be around 30 μm by adjusting the solid content in the coating solution. Meanwhile, as a supplementary experiment for understanding the phase inversion behavior in the coating solutions, a phase diagram for a ternary mixture comprising PVdF-HFP (polymer)/acetone (solvent)/water (nonsolvent) was investigated. The cloud points signifying a binodal curve of phase separation were measured by examining the precipitation of PVdF-HFP in the ternary mixture at room temperature. After dissolving a determined amount of PVdF-HFP in acetone, water (nonsolvent) was slowly added into the PVdF-HFP solution until the solution became permanently turbid, revealing the precipitation of PVdF-HFP.

The air permeability, microporous structure, and thermal shrinkage of separators are the major characteristics to be carefully monitored. In particular, the air permeability represented by the Gurley value is considered a useful parameter to predict the ionic conductivity of separators, where a low Gurley value indicates high air permeability [1,14]. The air permeability was examined with a Gurley densometer (4110N, Gurley) by measuring the time necessary for air to pass through a determined volume under a given pressure. The surface morphology of the ceramic coating layers was investigated by field emission scanning electron microscopy (FE-SEM, S-4300, Hitachi). The thermal shrinkage of the ceramic composite separators was determined by measuring the dimensional change (area-based) of the separators after they were subjected to heat treatment at various temperatures for 0.5 h, where at least 5 samples per each separator were tested for securing the reproducibility. For the measurement of electrochemical performance, a liquid electrolyte of 1 M $LiPF_6$ in ethylene carbonate (EC)/diethyl carbonate (DEC) (1/1, v/v, Technosemi Chem) was employed. The ionic conductivity of the separators was obtained by AC impedance analysis using a reference600 response analyzer (Gamry Instruments) over a frequency range of 1–10^6 Hz. A lithium half-cell (2032-type coin cell) was assembled by sandwiching the separator between a lithium-metal anode and a $LiCoO_2$ cathode and then activated by filling the liquid electrolyte. All assembly of cells was carried out in an argon-filled glove box. The discharge C-rate capability of the cells was examined using battery test equipment (PNE Solution), where the discharge C-rates were varied from 0.2 C (=0.68 mA cm^{-2}) to 2.0 C (=6.81 mA cm^{-2}) at a constant charge C-rate of 0.2 C under a voltage range between 3.0 V and 4.3 V.

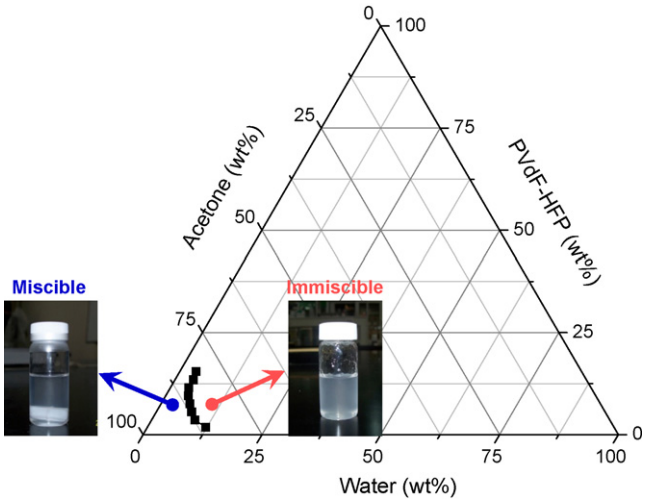

Fig. 1. A phase diagram for a ternary mixture comprising PVdF-HFP (polymer)/acetone (solvent)/water (nonsolvent). Photographs for a miscible coating solution (water content = 2 wt%) and an immiscible coating solution (water content = 10 wt%) are inserted.

3. Results and discussion

As a first step to understanding the phase inversion behavior that determines the microporous structure of ceramic coating layers, a phase diagram for a ternary mixture comprising PVdF-HFP/acetone/water was investigated (Fig. 1). When the critical amount of water to induce the phase separation is added into PVdF-HFP/acetone solutions, PVdF-HFP precipitates, causing the transparent solution to become turbid. Photographs for the coating solutions with different water contents show that the solution with a low water content belonging to a miscible region in the phase diagram is transparent, whereas the solution with a high water content belonging to an immiscible region is opaque (Fig. 1). The precipitation points signifying the phase separation were observed preferentially at the solvent-rich and nonsolvent-poor regions. This demonstrates that water is a strong enough nonsolvent to disturb the system equilibrium and induce the PVdF-HFP precipitation in the solution.

On the basis of this phase diagram, the mechanism of microporous structural development in the ceramic coating layers is discussed. As a preliminary step, an investigation on the pristine PVdF-HFP coating layers without Al_2O_3 powders was conducted. When the coating solution consisting of PVdF-HFP/acetone/water is cast onto a PE separator, water acts as a nonsolvent to induce the phase separation while acetone is evaporating. During the evaporation of the acetone, the initially transparent cast layers gradually become opaque and solidified, demonstrating that the microporous structures in the coating layers are formed by the phase inversion [15,16]. The effect of water content on the morphology of the PVdF-HFP coating layers was examined at a fixed PVdF-HFP concentration of 6 wt%. Fig. 2 demonstrates that as the water content increases, that is, as the initial composition of the coating solutions proceeds further into an immiscible region, the pore size of the resulting PVdF-HFP coating layers becomes larger and the porous structure becomes more developed, which verifies that the nonsolvent (water) is effective in inducing the phase inversion. Based on these results for the PVdF-HFP coating layers, the morphology of Al_2O_3/PVdF-HFP (=50/50, w/w) ceramic coating layers was then examined as a function of the water content in the coating solutions.

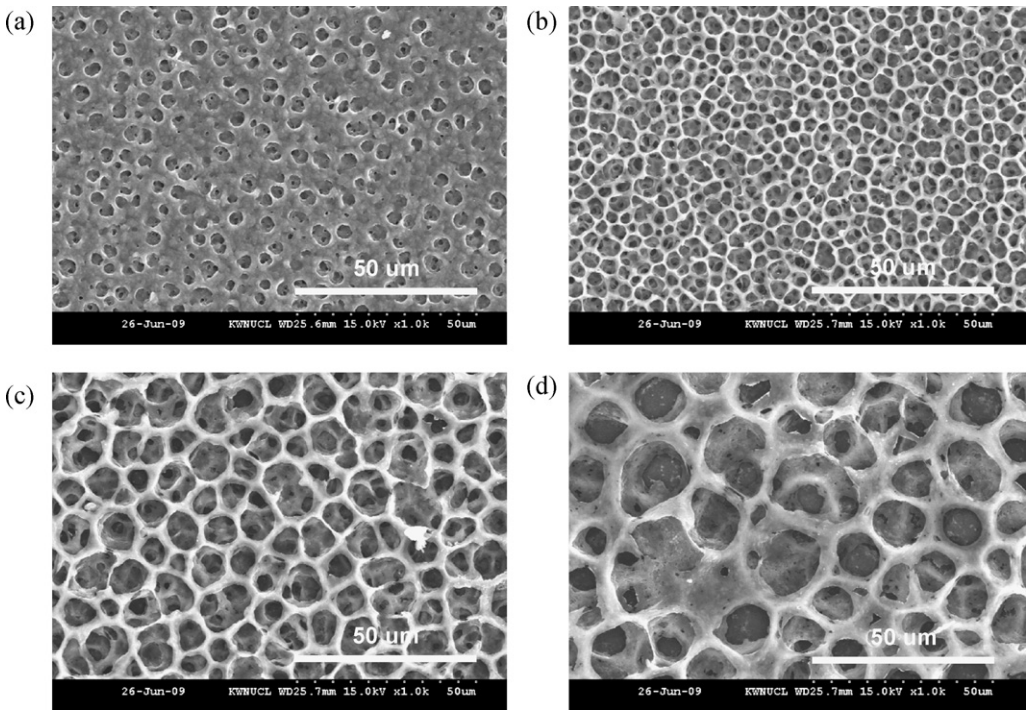

Fig. 2. FE-SEM photographs for PVdF-HFP coating layers without Al_2O_3 powders as a function of water content in coating solutions: (a) 2 wt%; (b) 4 wt%; (c) 6 wt% and (d) 8 wt%.

Fig. 3 shows that the Al_2O_3 powders are well-mixed with the PVdF-HFP binders and that the micropores were developed in the coating layers. Notably, as the water content increases, the microporous structure of the ceramic coating layers becomes more developed. This demonstrates that, similarly to the PVdF-HFP coating layers, the microporous structure development in the Al_2O_3/PVdF-HFP ceramic coating layers strongly depends on the phase inversion.

To quantitatively analyze the microporous structures of the coating layers, the air permeability represented by Gurley value was examined. Fig. 4 shows the Gurely values of composite separators as a function of water content. As the water content in the coating solutions increases, the Gurley values of the separators tend to decrease; that is, the air permeability increases, which demonstrates that a tortuous path for air transport becomes shorter [14].

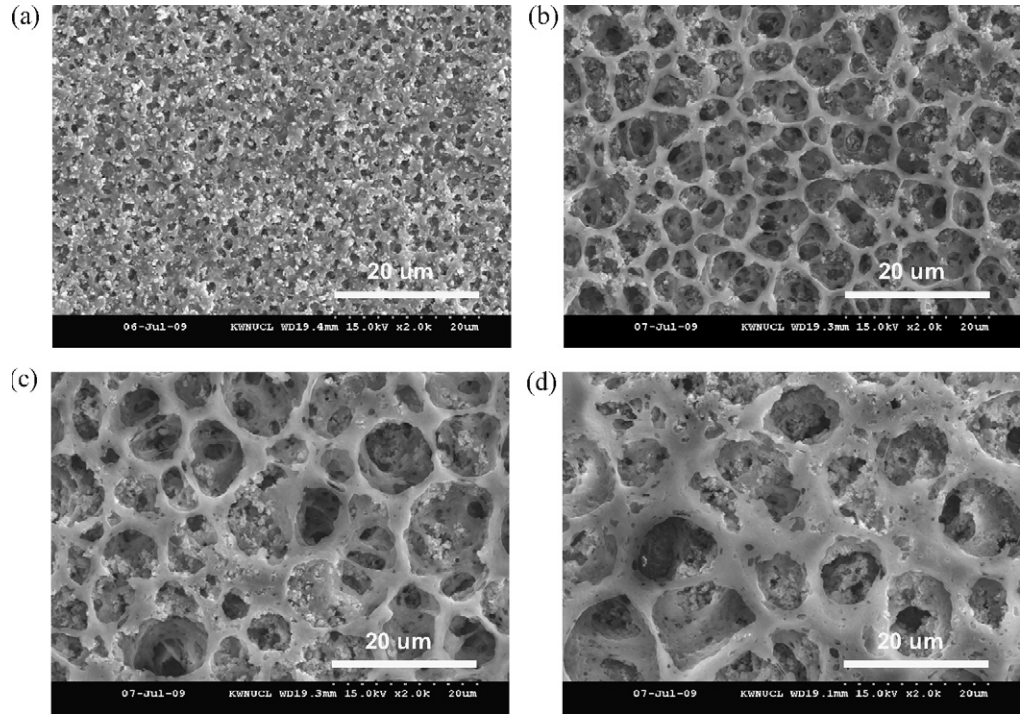

Fig. 3. FE-SEM photographs for Al_2O_3/PVdF-HFP (=50/50, w/w) ceramic coating layers as a function of water content in coating solutions: (a) 1.89 wt%; (b) 3.77 wt%; (c) 5.66 wt% and (d) 7.55 wt%.

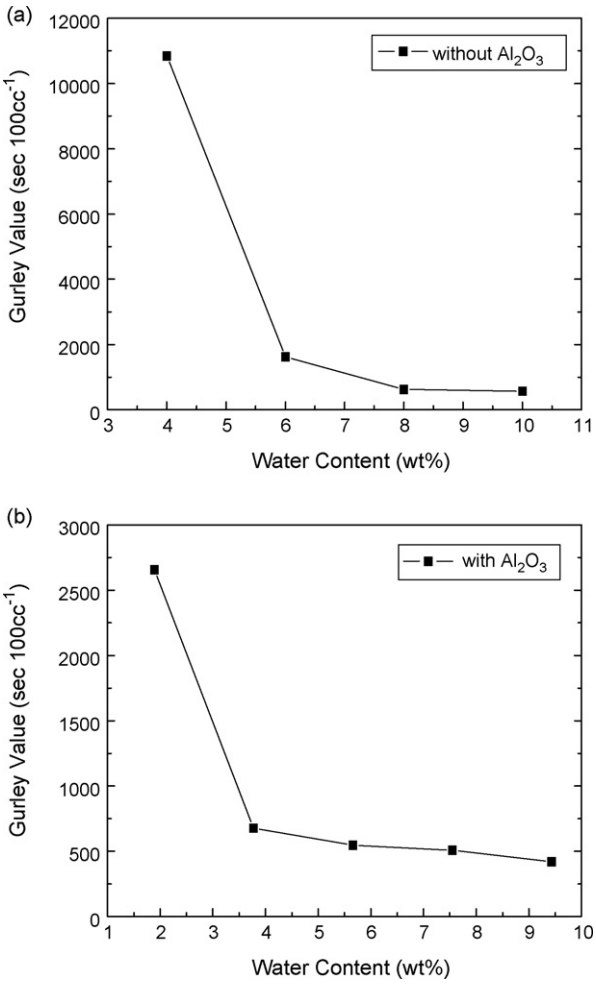

Fig. 4. Dependence of Gurley values of composite separators on water content: (a) composite separators without Al_2O_3 powders and (b) composite separators with Al_2O_3 powders.

Meanwhile, compared to the PVdF-HFP coating layers (Fig. 4(a)), the Al_2O_3/PVdF-HFP ceramic coating layers (Fig. 4(b)) show the lower Gurley values, which suggests that the incorporation of Al_2O_3 powders in the coating layers allows a more developed porous structure, contributing to the facile air transport. Another noteworthy observation is that the decrease in the Gurley values is not

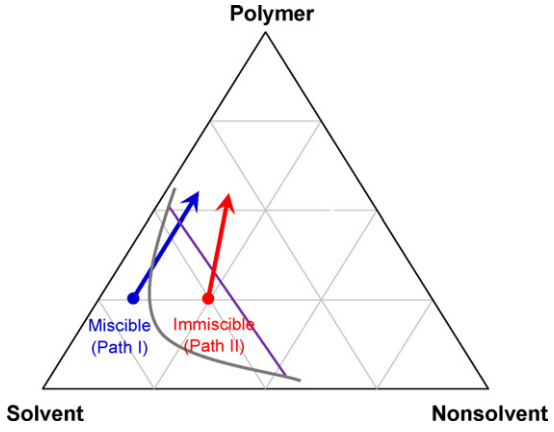

Fig. 5. Schematic representation for dependence of drying path on initial composition of coating solution: miscible solution (path I) and immiscible solution (path II).

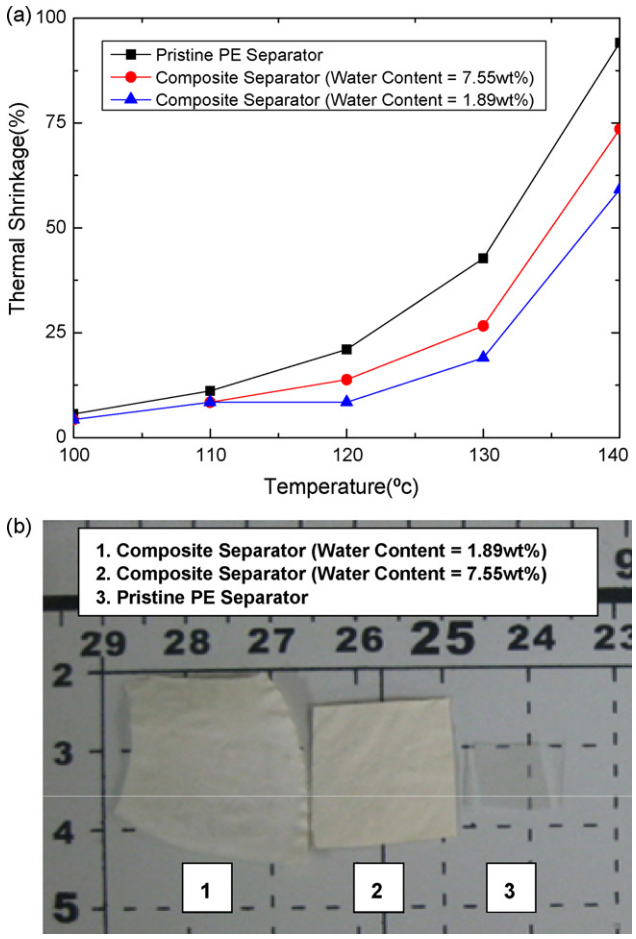

Fig. 6. (a) Thermal shrinkage of composite separators and pristine PE separator as a function of heat treatment temperature; (b) photographs of ceramic composite separators and pristine PE separator after heat treatment at 140 °C and 0.5 h.

linearly proportional to the increase in the water content. Fig. 4 reveals that the relative change in the Gurley values with the addition of water is steep in the region of low water contents, and flattens in the region of high water contents. This interesting behavior of Gurley values can be explained by considering the phase diagram for the ternary mixture of PVdF-HFP/acetone/water. On the basis of the phase diagram shown in Fig. 1, the dependence of drying path on the initial composition of coating solution is schematically represented in Fig. 5. This demonstrates that whether the initial composition of solution belongs to a miscible region or an immiscible region would be an important factor to govern the drying path of solution (paths I and II in Fig. 5). As solvent evaporates, the coating solution goes through phase separation and splits into a polymer-rich phase (polymer backbones in membranes) and a polymer-poor phase (pores in membranes), where the relative amount of each phase depends on the lever rule of the tie line [17,18]. For instance, when an initial composition of coating solution belongs to a miscible region, the phase separation may proceed preferentially along the nonsolvent-poor region in the phase diagram (path I in Fig. 5). According to the lever rule of the tie line, this phase separation generates a small amount of polymer-poor phase. The small amount of polymer-poor phase reflects the poor development of microporous structure, which yields the high Gurley values, that is, the low air permeability. Between two coating solutions with different water contents, the difference in the amount of polymer-poor phase is large particularly in a miscible region, whereas it is relatively small in an immiscible region. The understanding of this interesting phase separation behavior explains the

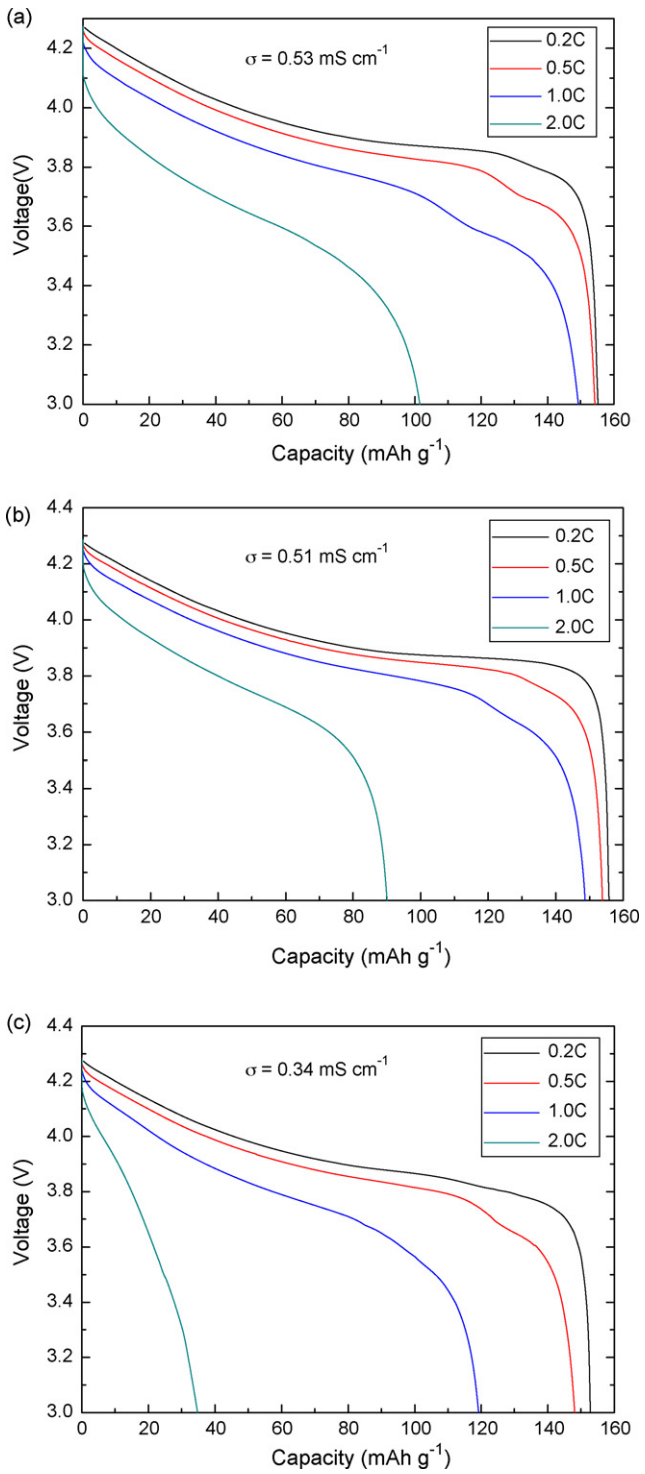

Fig. 7. Discharge profiles of cells with: (a) pristine PE separator and (b) composite separator (water content = 7.55 wt%); (c) composite separator (water content = 1.89 wt%), where discharge C-rate is varied from 0.2 C (=0.68 mA cm^{-2}) to 2.0 C (=6.81 mA cm^{-2}) at a constant charge C-rate of 0.2 C under a voltage range between 3.0 V and 4.3 V.

unique change in the Gurley value that is found to be not linearly proportional to the water contents in the coating solutions.

The thermal shrinkage of ceramic composite separators was observed by measuring the dimensional change (area-based) of the separators after they were subjected to heat treatment at various temperatures for 0.5 h. Fig. 6 shows that the ceramic composite separators have better thermal shrinkage than the pristine PE separator over a wider range of temperatures, which verifies that the introduction of ceramic coating layers is effective in improving the thermal shrinkage of separators. The thermal shrinkage of ceramic composite separators was further examined as a function of coating solution miscibility. The water contents of 1.89 wt% and 7.55 wt% were respectively chosen as representative examples for a miscible coating solution and an immiscible coating solution. Notably, the miscible coating solution exhibits the better thermal shrinkage than the immiscible coating solution. At a temperature of 140 °C, the thermal shrinkage of the ceramic composite separators was observed to be about 59% for the miscible coating solution and 74% for the immiscible coating solution, compared to 94% for the pristine PE separator. This improvement in the thermal shrinkage for the miscible coating solution can be attributed to the relatively compact structure of the ceramic coating layers. As previously observed, the miscible coating solution yields the poor development of microporous structure and the high Gurley values. This relatively dense structure of the ceramic coating layers is expected to effectively prevent the separators from being thermally shrunk.

As a final step, the effect of phase inversion, that is, of the water contents in the coating solutions, on electrochemical performances such as ionic conductivity and discharge C-rate capability of separators was examined. For making a clear comparison, the water contents of 1.89 wt% and 7.55 wt% were respectively chosen as representative examples for a miscible coating solution and an immiscible coating solution. Fig. 7 demonstrates that the discharge C-rate capability of the immiscible coating solution (water content = 7.55 wt%) appears to be comparable to that of the pristine PE separator, which reveals that the ceramic coating layer prepared from the immiscible coating solution does not significantly hinder the ionic conduction owing to its well-developed porous structure. Another important observation is that the immiscible coating solution shows the better discharge C-rate capability than the miscible coating solution. The difference in the discharge C-rate capacity between the two coating solutions becomes larger particularly at the higher C-rates where the influence of ionic transport on the ohmic polarization (i.e. IR drop) is more important. Previous observations found that the immiscible coating solution presents the highly developed porous structures and the low Gurley values. The Gurley value is known to be a quantitative indicator to predict the ionic conductivity of a separator [1,6]. Fig. 7 also includes a comparison of the ionic conductivities of the two separators prepared from the different coating solutions, which respectively shows 0.34 mS cm^{-1} for the miscible coating solution and 0.51 mS cm^{-1} for the immiscible coating solution. Therefore, for the separator prepared from the immiscible coating solution, this facile ionic transport allows the superior discharge C-rate capability.

A future study will focus on the dependence of phase inversion on solvent/nonsolvent miscibility and its influence on the thermal shrinkage and the electrochemical performance of ceramic composite separators.

4. Conclusions

We successfully developed a new composite separator with remarkably improved thermal shrinkage by introducing microporous ceramic coating layers (Al_2O_3/PVdF-HFP) onto a PE separator. A pre-investigation on the phase inversion for the ternary mixture (PVdF-HFP/acetone/water) provided a theoretical basis for controlling the microporous structure of coating layers. As the water content in the coating solution increases, that is, as the coating solution goes further into the immiscible region in the phase diagram, the resulting coating layer becomes more porous and the Gurley value decreases. Based on the observation of this phase inversion behavior, the thermal shrinkage and electrochemical performance of the separators were examined as a function of the

coating solution miscibility. A noteworthy observation is that the immiscible coating solution presents the superior electrochemical performance, whereas the miscible coating solution shows the better thermal shrinkage. The important contribution of this study is to demonstrate that the variation of nonsolvent content in the coating solution based on the understanding of the phase inversion is an effective way to control the microporous structure in the ceramic coating layers, which crucially affects the thermal shrinkage as well as the electrochemical performance of the ceramic composite separators.

Acknowledgments

This work was supported by National Research Foundation of Korea Grant funded by the Korean Government (KRF-2008-331-D00150) and MKE & IITA through IT Programs. We are grateful to Dr. E.K. Shim and Mr. J.S. Kim at TechnosemiChem, Mr. S.H. Kim at Arkema Korea, and Mr. B.J. Choi at ExxonMobil Korea for their supply of samples. We also express deep appreciation to Mr. W.J. Kim and Prof. S.M. Lee at Kangwon National University, Dr. K.J. Kim and Mr. Y.N. Cho at KETI for their kind assistance in the characterization of electrochemical performance.

References

[1] P. Arora, Z. Zhang, Chem. Rev. 104 (2004) 4419.
[2] K.M. Abraham, M. Alamgir, D.K. Hoffman, J. Electrochem. Soc. 142 (1995) 683.
[3] Z. Jiang, B. Carroll, K.M. Abraham, Electrochim. Acta 42 (1997) 2667.
[4] K.M. Abraham, Z. Jiang, B. Carroll, Chem. Mater. 9 (1997) 1978.
[5] S.S. Zhang, K. Xu, T.R. Jow, J. Power Sources 140 (2005) 361.
[6] T. Takemura, S. Aihara, K. Hamano, H. Yoshiyasu, J. Power Sources 146 (2005) 779.
[7] S. Augustin, V. Hennige, G. Hoerpel, C. Hying, Desalination 146 (2002) 23.
[8] W. Yi, Z. Huaiyu, H. Jian, L. Yun, Z. Shushu, J. Power Sources 189 (2009) 616.
[9] T.H. Cho, M. Tanaka, H. Onishi, Y. Kondo, T. Nakamura, H. Yamazaki, S. Tanase, T. Sakai, J. Power Sources 181 (2008) 155.
[10] C. Yang, Z. Jia, Z. Guan, L. Wang, J. Power Sources 189 (2009) 716.
[11] Y.M. Lee, J.W. Kim, N.S. Choi, J.A. Lee, W.H. Seol, J.K. Park, J. Power Sources 139 (2005) 235.
[12] K.M. Kim, N.G. Park, K.S. Ryu, S.H. Chang, Electrochim. Acta 51 (2006) 5636.
[13] Y.J. Hwang, K.S. Nahm, T.P. Kumar, A.M. Stepha, J. Membr. Sci. 310 (2008) 349.
[14] S.S. Zhang, J. Power Sources 164 (2007) 351.
[15] M.L. Yeow, Y.T. Liu, K. Li, J. Appl. Polym. Sci. 90 (2003) 2150.
[16] W. Pu, X. He, L. Wang, C. Jiang, C. Wan, J. Membr. Sci. 272 (2006) 11.
[17] M. Mulder, Basic Principles of Membrane Technology, Kluwer Academic Publishers, London, 1996.
[18] I.C. Kim, H.G. Yun, K.H. Lee, J. Membr. Sci. 199 (2002) 75.